Molecular and Cellular Biochemistry (2023) 478:1813–1824
https://doi.org/10.1007/s11010-022-04632-9

Investigation of effects of transferrin-conjugated gold nanoparticles on hippocampal neuronal activity and anxiety behavior in mice

Yavuz Yavuz[1] · Gamze Yesilay[2] · Bilge Guvenc Tuna[3] · Akif Maharramov[3] · Mustafa Culha[4,5] · Cihan Suleyman Erdogan[1] · Gunseli Ayse Garip[6] · Bayram Yilmaz[1]

Received: 18 September 2022 / Accepted: 3 December 2022 / Published online: 27 December 2022

Abstract

Gold nanoparticles (GNPs) have been widely used in medicine such as imaging, drug delivery and therapeutics due to their multifunctional properties. Alterations in neuronal function may contribute to various neurological diseases. Transferrin plays a primary role in iron transportation and delivery and has recently been utilized for drug delivery to the brain. We have investigated effects of transferrin-conjugated GNPs (Tf-GNPs) on anxiety and locomotor behavior in vivo and also hippocampal neuronal activity ex vivo. Electrophysiological effects of Tf-GNP on hippocampal neurons were determined by patch clamp method. Fifteen male young adult C57BL/6 mice were randomly divided into three groups as control (200 µL PBS), GNP (bare GNP; 2.2 µg/g in PBS) and Tf-GNPs (2.2 µg/g Tf-GNP). Animals intraperitoneally received the respective treatments for seven consecutive days and were subjected to elevated plus maze (EPM) and open field tests (OFT). Ex vivo, firing frequency of the neurons significantly increased by GNP treatment ($p < 0.001$). In vivo, animals in Tf-GNP group showed significantly longer distance in open arms but significantly lower number of entries to the open arms in EPM ($p < 0.05$). Mice received bare GNPs had significantly higher locomotor activity in OFT ($p < 0.05$), while Tf-GNP did not alter the locomotor activity significantly ($p = 0.051$). Animals in Tf-GNP group spent significantly longer time in the peripheral zone in OFT ($p < 0.05$). The present findings have shown that Tf-GNP induces anxiety-like behavior without altering spontaneous firing rate of hippocampal neurons. We suggest that neurobiological effects of Tf-GNP should be predetermined before using in medical applications.

Keywords Action potential · Anxiety-like behaviors · Electrophysiology · Gold nanoparticles · Locomotor activity · Transferrin

Introduction

Gold nanoparticles (GNPs) are preferred in biological applications compared to other nano-structured materials due to their high biocompatibility and low toxicity properties to cells [1]. They are used especially in gene and drug transport, cancer treatment, imaging technologies and neurological diseases due to their ability to penetrate into tissue easier and stimulate the immune system less [1–3]. Moreover, they are being developed for various other applications as diagnostics [4–6], thermal [7–9], radiation [10, 11] and photodynamic therapy against cancer [11, 12]. The chance of regulating nanoparticle characteristics such as physical, chemical, and biological properties brings up several opportunities to use these nanoparticles in diagnostic drug delivery studies [13]. In addition, the changes in photoacoustic

✉ Bayram Yilmaz
byilmaz@yeditepe.edu.tr

1 Department of Physiology, Faculty of Medicine, Yeditepe University, Istanbul, Turkey

2 Department of Molecular Biology and Genetics, Hamidiye Institute of Health Sciences, University of Health Sciences-Turkey, Istanbul, Turkey

3 Department of Biophysics, Faculty of Medicine, Yeditepe University, Istanbul, Turkey

4 Department of Chemistry and Physics, Augusta University, Augusta, GA, USA

5 Nanotechnology Research and Application Center (SUNUM), Sabanci University, Istanbul, Turkey

6 Department of Biophysics, School of Medicine, Marmara University, Istanbul, Turkey

and photothermal properties and allows the use of light of different wavelengths in therapy [9].

It is thought that changes in action potential, which is the most basic and important feature of excitable cells, can lead to neurological diseases such as epilepsy [14], pain sensation [15] and psychiatric disorders [16]. Several exogenous factors (such as anesthetics and toxicants) and neuromodulators have been reported to affect neuronal excitability [17–20]. Therefore, it is important to determine possible functional changes can be caused by GNPs to be used in medical applications in neurons and that these changes may be prevented with different surface coating strategies [21].

The blood brain barrier (BBB), which plays an important role in maintaining brain homeostasis, may prevent drugs from reaching the brain in the treatment of cancer and neurological diseases due to its selective permeability [22]. However, molecules such as insulin, leptin, insulin-like growth factor 1 and transferrin in the plasma can pass the BBB by a carrier-mediated method [23, 24]. Transferrin is a 76-kDa glycoprotein primarily produced in liver in humans and plays important roles in iron delivery throughout the body via incorporation through transferrin receptor 1-mediated endocytosis [25]. Since transferrin and transferrin receptor system show specific properties in the brain endothelium, transferrin is more suitable for the development of carrier systems in targeting the brain [26].

Effects of transferrin-conjugated GNPs (Tf-GNPs) on central nervous system neuronal activity and plasticity are not known yet. Therefore, in this study, we aimed to investigate effects of bare GNPs and Tf-GNPs on neural activity using in vivo behavior and ex vivo electrophysiology models. We showed that, bare GNPs, but not the Tf-GNPs, elevated the spontaneous firing frequency of hippocampal neurons ex vivo. In addition, Tf-GNPs elevated the anxiety-like behavior without altering the locomotor activity in vivo. As a result, the use of Tf-GNPs suggested as less neurotoxic for bioapplications but using bare GNPs should considered more carefully.

Methods

Preparation of gold nanoparticles

Synthesis of gold nanoparticles

GNPs of 13 nm diameter size were synthesized by Turkevich's citrate reduction method. Briefly, a 200 mL aqueous solution of HAuCl4·3H2O (1.1 mM; Sigma-Aldrich, #G4022-5G) was boiled on a magnetic stirrer at 1000 rpm. Once boiled, a 10 mL of 38.8 mM sodium citrate dehydrate (Merck Millipore, #1064321000) was immediately injected and the mixture was boiled for another 15 min. The colloid was left at room temperature for cooling down before using in further experiments.

Transferrin conjugation of gold nanoparticles

GNP surfaces were first modified with cysteamine. A 100 µM (200 µL) solution of cysteamine was added to 13 mL of GNP colloid and left under vigorous shaking at room temperature overnight. Then, N-(3-Dimethylaminopropyl)-N'-ethylcarbodiimide hydrochloride (EDC; Merck Millipore, #00907)/N-Hydroxysuccinimide (NHS; Sigma-Aldrich, # 130672) coupling reaction was initiated by addition of EDC and NHS to a final concentration of 1.6 µM EDC, 1.6 µM NHS and 1.6 µM apo-transferrin human (Sigma-Aldrich, #T4382-500MG) to 10 mL of cysteamine-modified GNPs. The reaction continued for 24 h by shaking at room temperature. To remove unbound transferrin and chemicals, the colloid was washed three times with deionized water and centrifuged 3×15 min at 18,000×g.

Characterization of gold nanoparticles

Characterization of bare GNPs and Tf-GNPs were conducted using a UV–Vis spectrophotometer (Lambda 25, PerkinElmer, USA), dynamic light scattering (DLS) and zeta potential measurements (ZetaSizer Nano ZS, Malvern Panalytical, UK). All experiments were performed in the water dispersant state at 25 °C. Three repeats for each sample were conducted to estimate the standard deviation in the measurements. TEM images of bare GNP and Tf-GNPs were obtained using a standard carbon grid with Jeol JEM-2100 Plus Electron Microscopy (Japan) in Yeditepe University. FTIR spectra were obtained using Thermo Scientific Nicolet iS50 instrument with ATR module.

In vitro toxicity of bare gold nanoparticles and transferrin-conjugated gold nanoparticles

GT1-7 cells that are mouse immortalized gonadotropin-releasing hormone neurons [27] were used to investigate the in vitro toxicity of bare GNPs and Tf-GNPs. The GT1-7 cells were routinely maintained in DMEM (Gibco; 10569010) supplemented with 10% heat-inactivated fetal bovine serum (Gibco, 10500) and penicillin/streptomycin/neomycin (50 µg/mL/50 µg/mL/100 µg/mL) mixture (Gibco, 15640055) at 37 °C under 5% CO_2 humidified atmosphere. For in vitro toxicity experiments, 1×10^5 cells in 500 µL/well were seeded in a 24-well plate. After overnight attachment cells were treated with either bare or transferrin-conjugated GNPs at the doses of 5, 10, 25, 50 and 100 nM for 24 h. Cell viability were determined using trypan blue dye exclusion assay [28] and counted on an automated cell counter (Countess™ 3 Automated Cell Counter, Thermo Fisher Scientific).

The cell counts were then normalized against the respective control group and expressed as percent of control.

Determining the amount of GNP and Tf-GNP accumulated in mice brains

To determine the brain uptake of bare GNP and Tf-GNP in mice, inductively coupled plasma mass spectrometry (ICP-MS; Perkin-Elmer Nexion 300XX) was used with nickel sampler and skimmer cones 3 days after injection ($n = 3$/group). A microwave digestion system, Titan MPS Microwave Sample Preparation System (PerkinElmer, USA), with a rotor for sixteen Teflon digestion vessels was used for sample digestion process. Whole mice brains were homogenized and used for measurements.

Brain slice preparation, electrophysiology and patch clamp

Slice preparation was performed as described previously [29]. Briefly, C57BL/6 mice were sacrificed and brains were immersed in *N*-Methyl-D-glucamine (NMDG)-HEPES containing artificial cerebrospinal fluid (aCSF) cutting solution (92.0 mM NMDG, 2.5 mM KCl, 1.25 mM NaH_2PO_4, 30.0 mM $NaHCO_3$, 20.0 mM HEPES, 25.0 mM glucose, 2.0 mM thiourea, 5.0 mM Na-ascorbate, 3. mM Na-pyruvate, 0.5 mM $CaCl_2{\cdot}2H_2O$, and 10.0 mM $MgSO_4{\cdot}7H_2O$). Brain tissue was kept in 95% O_2/5% CO_2 aerated ice-cold cutting solution and 300 µm fresh slices containing the hippocampus were obtained with vibratome and transferred to 95% O_2/5% CO_2 aerated and HEPES containing artificial aCSF incubation solution (92.0 mM NaCl, 2.5 mM KCl, 1.25 mM NaH_2PO_4, 30.0 mM $NaHCO_3$, 20.0 mM HEPES, 25.0 mM glucose, 2.0 mM thiourea, 5.0 mM Na-ascorbate, 3.0 mM Na-pyruvate, 2.0 Mm $CaCl_2{\cdot}2H_2O$, and 2.0 mM $MgSO_4{\cdot}7H_2O$). The sections were incubated in this solution for at least 1 h and placed in the recording chamber which had the recording aCSF solution (124 mM NaCl, 2.5 mM KCl, 1.25 mM NaH_2PO_4, 24 mM $NaHCO_3$, 12.5 mM glucose, 5.0 mM HEPES, 2.0 mM $CaCl_2{\cdot}2H_2O$, and 2.0 mM $MgSO_4{\cdot}7H_2O$). Cell-attached loose-seal recordings were performed in voltage clamp mode and action currents were recorded from hippocampal neurons using electrodes with 4–5 MΩ tip resistances. Recording aCSF was used as the pipette solution for cell-attached recordings. MultiClamp 700B Amplifier (Molecular Devices, San Jose, CA) and Axon™ pCLAMP™ 11.3 software (Molecular Devices, San Jose, CA) were used to obtain and analyze the data. After a sufficient amount of control recordings were taken from the brain slices, bare GNP (0.01 mM) and Tf-GNPs (0.01 mM) were added into the bath through perfusion and taken population recordings.

Experimental setup and in vivo experiments

Fifteen male C57BL/6 mice (aged between 4 and 6 weeks) were obtained from Yeditepe University Medical School Experimental Research Center (YUDETAM). They were housed under controlled temperatures (21 ± 1 °C) and lighting conditions (12/12-h light/dark cycle). Standard mice chow and tap water were provided ad libitum. Experimental procedures were approved by the Yeditepe University experimental animal research ethics committee (Number: 599, Date: 30.03.2017).

Animals were randomly divided into three groups as control, GNP and Tf-GNP groups ($n = 5$ animals in each group). For seven consecutive days, animals in control, GNP and Tf-GNP groups were administered with PBS (200 µL), bare GNP (2.2 µg/g body weight in 200 µL PBS) and Tf-GNP (2.2 µg/g body weight in 200 µL PBS) intraperitoneally. At the end of the administration period, behavioral effects of GNP and Tf-GNP were examined.

Elevated plus maze

The elevated plus maze (EPM) test measures anxiety-like behavior in mice [30]. Mice were individually placed in the central-open area within the EPM. Testing was done for 5 min. Mice were placed into a Plexiglass chamber, which was with a height of 50 cm from the ground consisted of plus-shaped arms (length: 50 cm, width: 10 cm) and consisted of a labyrinth with open and closed areas. Scoring was based on time spent in the open versus close arms and entries into the close versus open arms. Behavior was recorded using the EthoVision system (Noldus).

Open field test

The open field test (OFT) was used to assess locomotion and anxiety-like behavior in mice as previously reported [31]. Locomotor activity of all mice was measured after the injection at the end of seven days by OFT to determine the anxiety-like behavior of the animals. Mice were placed into a Plexiglass chamber (length x width x height = 60 cm × 60 cm × 42 cm) and allowed to acclimate to the chamber for about 3 min. Their activity was tracked for 10 min ($n = 7$ mice). The total distance traveled, the number of crossings into the middle portion of the area (center quadrant, 20 cm × 20 cm), total time spent in the center and corners, and velocity were determined by offline analysis (EthoVision, Noldus).

Statistical analysis

Data were analyzed using GraphPad Prism v7.0 (GraphPad Software, USA). Distribution of the data was examined

using Kolmogorov–Smirnov test. Data of two dependent groups were analyzed using Student's paired *t* test in case of the data were normally distributed. Data of groups with normal distribution were analyzed using One-Way analysis of variance (One-way ANOVA) followed by Tukey's multiple comparison tests or two-way ANOVA followed by multiple comparison tests. The data without normal distribution were analyzed with Kruskal–Wallis, followed by Dunn's multiple comparison tests. $P < 0.05$ was considered to be statistically significant. Data were represented as mean ± standard deviation.

Results

Characterization of GNPs

The UV–Vis spectroscopy of bare GNPs and Tf-GNPs revealed peak maxima at 519 nm and 528 nm, respectively (Fig. 1a). DLS measurements resulted in that the mean diameter of the bare GNPs were 13.54 ± 3.73 nm (min–max = 8.7–37.8 nm), while the mean diameter of the transferrin-conjugated GNPs was 30.44 ± 6.64 nm (min–max = 21.04–68.06 nm; Fig. 1b). The zeta potentials of bare GNP and Tf-GNP were -26.17 ± 2.15 mV and -28.00 ± 0.55 mV, respectively ($p = 0.22$). TEM image measurements were similar to the DLS measurements with the mean diameter of the bare GNPs were 13.09 ± 4.36 (Fig. 2a) and the mean diameter of the transferrin-conjugated GNPs was 17.9 ± 8.3 nm (Fig. 2b). The change in the diameter size of the particles proves the successful conjugation of transferrin protein. To confirm Tf conjugation to GNPs, FTIR spectra of both bare and Tf-conjugated GNPs were obtained (Fig. 3a, b). As a comparison, FTIR spectra of sodium citrate (Fig. 3c) that has been used in GNP synthesis as well as commercial powder of Tf (Fig. 3d) used in conjugation were obtained. Compared to bare GNPs, a slight increase in protein Amide region in GNP-Tf was observed at 1663 cm^{-1}. Although all the characterizations of GNPs were performed in water, their stability might be different in PBS. There are studies reported that citrate stabilized gold nanoparticles might not be stable in physiological environment [32, 33].

In vitro toxicity of GNPs

Bare and Tf-conjugated GNPs did not cause any morphological alterations in vitro (Fig. 4a). Moreover, none of the GNPs showed toxic effects on GT1-7 cells (Fig. 4b).

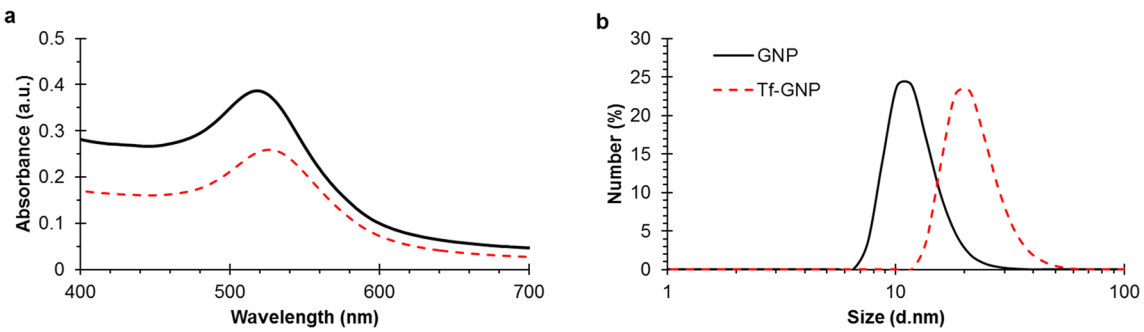

Fig. 1 Physical characteristics of bare GNPs and Tf-GNPs. **a** UV/Vis spectrum and **b** size distribution in diameter by DLS

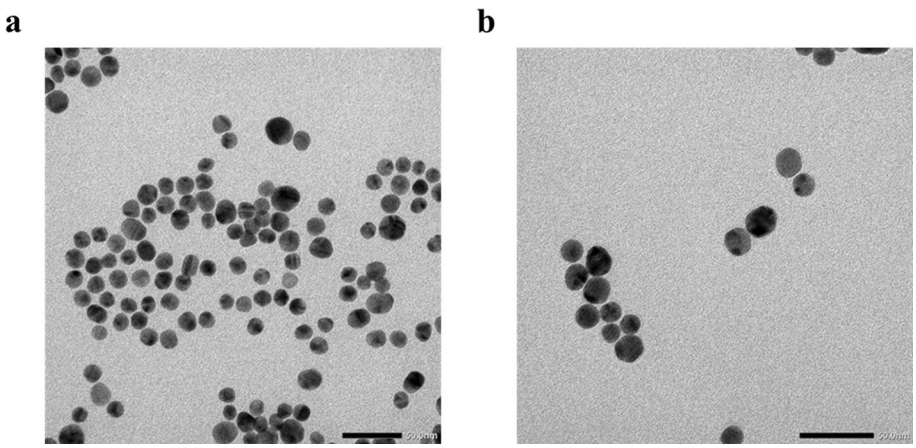

Fig. 2 TEM images of **a** bare GNPs and **b** Tf-GNPs. Particle size in diameter was 13.09 ± 4.36 before and 17.9 ± 8.3 after transferrin conjugation

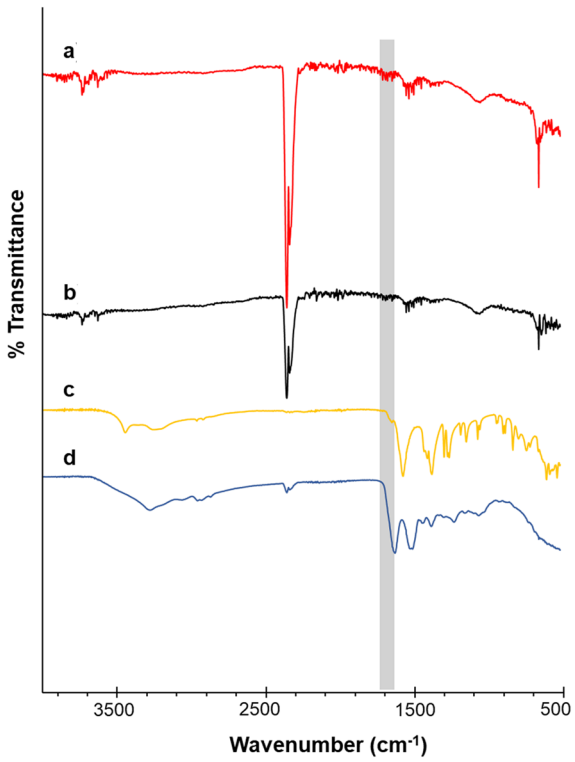

Fig. 3 FTIR spectra of conjugated and bare GNPs. FTIR spectra of (*a*) Tf-conjugated GNPs, (*b*) bare GNPs, (*c*) sodium citrate that has been used in GNP synthesis as a stabilizing and reducing agent, and (*d*) powder form Tf. The grey shaded area is the Amide region of Tf

The amount of GNP and Tf-GNP in mice brain

The amount of GNP three days after injection was determined by ICP-MS in mice brain. The GNP concentrations of brains of the mice administered with GNP (374.11 ± 5.03 ppb) and Tf-GNP (401.78 ± 35.12 ppb) were similar, indicating that the ability of the bare and Tf-GNP to cross the blood–brain barrier are similar (Fig. 5).

Electrophysiological effects of GNP and Tf-GNP on hippocampal neuronal activity ex vivo

We examined the electrophysiological effects of GNP and Tf-GNP upon the electrophysiological activity of hippocampal neurons ex vivo by patch clamp technique (Fig. 6a, b). GNP (0.01 mM) was applied to the bath mice brain slice ex vivo significantly increased the spontaneous firing frequency in hippocampal neurons compared to the control group ($p < 0.001$; Fig. 6c, d), while Tf-GNP caused no significant alterations in spontaneous firing frequency (Fig. 6c, d).

In vivo effects of GNP and Tf-GNP

Body weight and food intake

Body weight of the animals did not differ between the groups for seven days (Fig. 4a). However, animals received Tf-GNP had significantly higher food intake compared to the animals receiving bare GNP ($p < 0.05$) on day 4. However, on day 5, control group had significantly higher food intake in the control group of animals compared to the animals receiving bare GNP ($p < 0.05$), while there were no significant differences between GNP and Tf-GNP groups or control and Tf-GNP groups (Fig. 7b). Notably, there was a slight but significant decrease in the food intake in Tf-GNP group on day 5 compared to day 4 ($p < 0.05$; Fig. 7b), but there were no significant differences in food intake during the experimental period in other groups.

Anxiety-like behaviors determined by elevated plus maze

Animals received Tf-GNPs had significantly lower frequency of entry into open arms compared to closed arms ($p < 0.05$), while there were no differences in the animals in control and GNP groups with regards to the number of entries into both open and closed arms (Fig. 8a). The time spent in both arms did not significantly differ among the

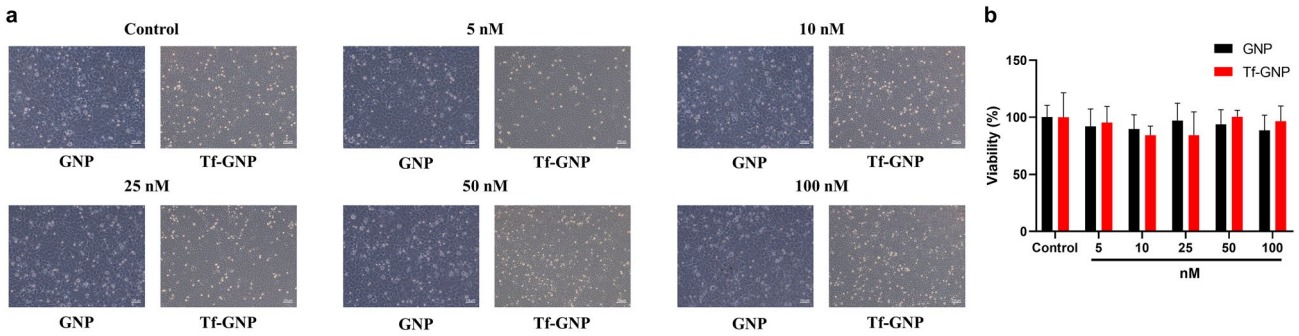

Fig. 4 In vitro toxicity of bare GNPs and Tf-GNPs. **a** Representative microscopy images and **b** viability of the cells

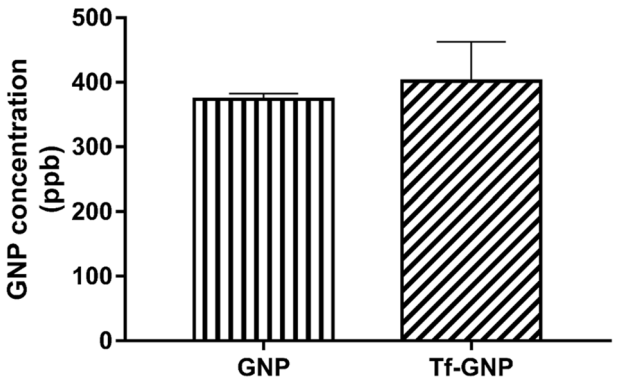

Fig. 5 Brain GNP and Tf-GNP concentrations. The concentration of gold (ppb) was measured in brain 3 days after injection of GNP and Tf-GNP (2.2 µg/g body weight in 200 µL PBS) intraperitoneally. Data are mean ± standard deviation. (Statistical analyses: Student's unpaired t-test)

groups (Fig. 8b). Tf-GNP group of animals had significantly higher mobility in the open arms compared to closed arms (**$p < 0.01$), however, there was no differences in mobility of the animals in control groups and animals that received bare GNP in both arms (Fig. 8c). On the other hand, mean speed of the animals during the experimental procedure was similar (Fig. 8d).

Locomotor activity and anxiety-like behaviors determined by open field

There were no significant differences between the groups in terms of total number of crossing the lines (Fig. 9a). Although there was a tendency of animals in all groups to spend time in the peripheral zone, only the animals in Tf-GNP group spent significantly higher time in the peripheral zone compared to central zone ($p < 0.01$; Fig. 9b). Animals received bare GNP traveled significantly higher distance ($p < 0.05$; Fig. 9c) and had a significantly higher mean speed ($p < 0.05$; Fig. 9d) compared to the control group of animals. However, although there was a tendency of the animals received Tf-GNP traveling longer distance and having a higher mean speed compared to control group of animals, the difference was not significant ($p = 0.051$; Fig. 9c, d).

Discussion

In the present study, we investigated the effects of transferrin-conjugated GNPs on spontaneous firing frequency ex vivo and on anxiety-like behavior and locomotor activity in vivo. In recent years, nanoparticles have gained attention for diagnostic, imaging, and therapeutic use due to their superior beneficial properties than traditional approaches. However, it has been reported they may exert neurotoxic effects [34–36]. Changes in the electrical activity of the neurons may lead to various neurological conditions, therefore, it is of great importance that nanoparticles to be used in medicine do not lead to alterations in neuronal function. As a noble metal, gold is more frequently preferred more because of its inertness, high biocompatibility and low toxicity [37, 38]. On the other hand, although the improvements in the synthesis procedures of GNPs, potential neurotoxic effects of GNPs are still present [39]. Therefore, altering the surface properties of GNPs is an alternative to prevent their adverse effects on neuronal functions and improve their beneficial activities in medicine.

Surface modifications of GNPs may both improve their bioavailability when brain is targeted [40] and may reduce the functional neurotoxicity [38]. In our study, we observed that transferrin conjugation of GNPs led to more negative, but not significantly, zeta potentials than bare GNPs. Previously, it was reported that the nanoparticles with more negative zeta potentials have a higher interaction with neurons and regulate the neuronal excitability in neural networks [41]. Apart from the zeta potential, physical adsorption which is happened as a results of high surface volume and instability of energy levels in surface atoms of nanoparticles might be the explanation of finding different effects of GNPs on firing frequency of neurons in vivo. The functional neurotoxicity studies in which GNPs were used are limited. It has been shown that star-shaped GNPs with an average size of 180 nm elevated the spontaneous firing frequency of hippocampal neurons via blocking K^+ channels [42]. In another study, different surface modifications of GNPs having different surface charges were tested on ex vivo hippocampal neurons and report variations at properties of action potentials of hippocampal neurons due to different surface charges [43]. A more recent study also showed the elevated spontaneous firing rate in hippocampal neurons when treated with bare GNPs [44]. In the present study, we also observed significantly higher spontaneous firing frequency in hippocampal neurons ex vivo when treated with bare GNPs. However, it has been reported they may exert neurotoxic effects [32–34]. Changes in the electrical activity of the neurons may lead to various neurological conditions, therefore, it is of great importance that nanoparticles to be used in medicine do not lead to alterations in neuronal function.

The hydrodynamic diameter change determined by DLS upon Tf conjugation indicates that Tf covers the GNP surface and created around 8.5 nm thick layer. The change in the diameter size of the particles indicates also the successful conjugation of transferrin protein. The slight increase of about 2 mV in zeta potential value shows that the particles are slightly more stable in colloidal form compared to bare GNPs. To confirm Tf conjugation to GNPs, FTIR spectra of both bare and Tf-conjugated GNPs were obtained and a slight increase in protein Amide region in GNP-Tf was

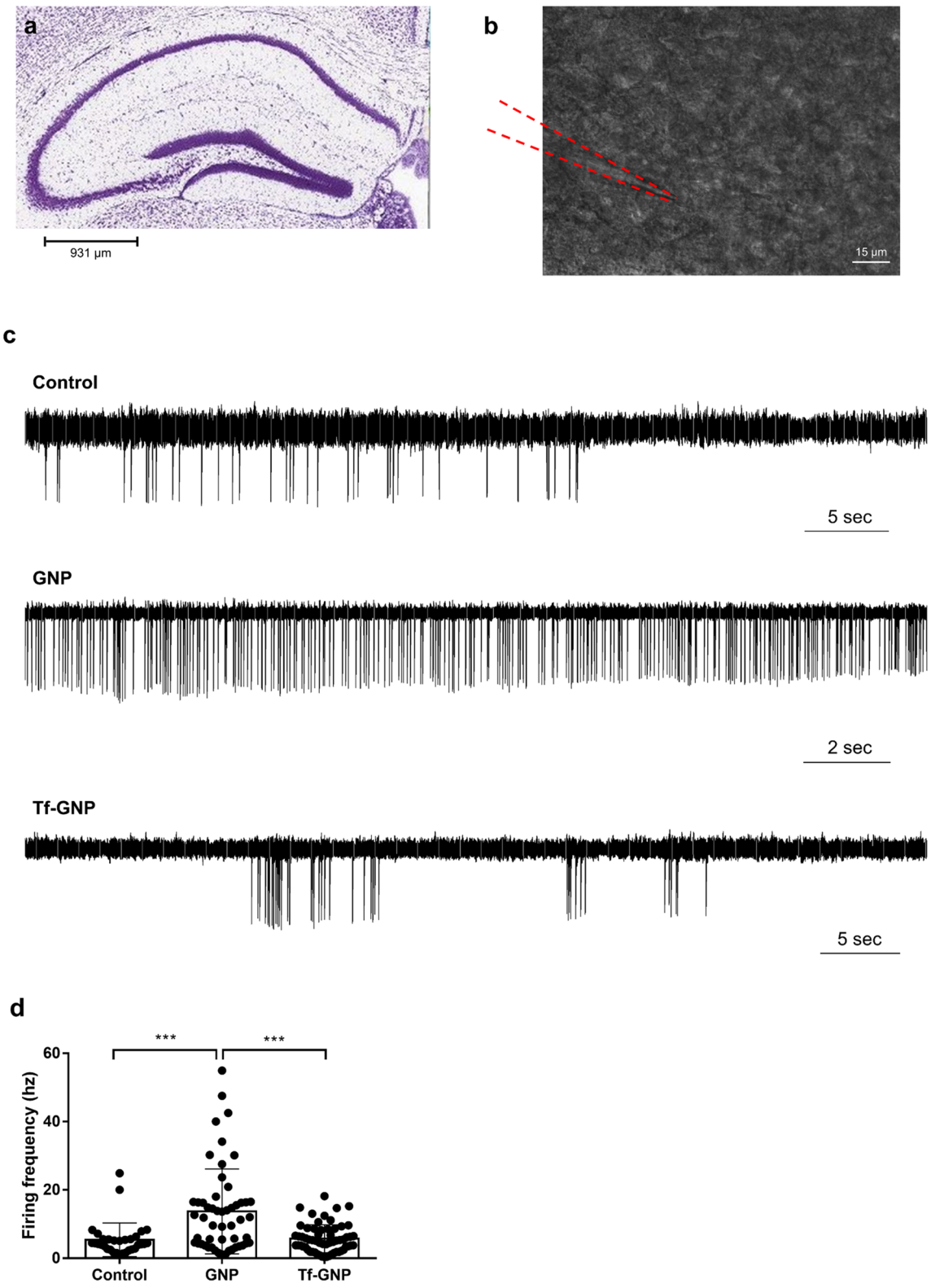

Fig. 6 Ex vivo effects of GNP and Tf-GNP on firing frequency of hippocampal neurons. **a** Representative image of hippocampus (Image credit: Allen Institute), **b** Representative image of cell-attached loose-seal recording from a hippocampal neuron (red dashed lines highlights the recording pipette), **c** representative cell-attached loose-seal recording traces for control, GNP and Tf-GNP groups and **d** effect of GNP and Tf-GNP on firing rate of hippocampal neurons. Each closed circle represents individual neurons (Control: $n=32$ neurons, GNP: $n=53$ neurons and Tf-GNP: $n=61$ neurons; recorded from slices from six mice; Statistical analysis: Kruskal–Wallis followed by Dunn's multiple comparison test. $^{***}p<0.001$)

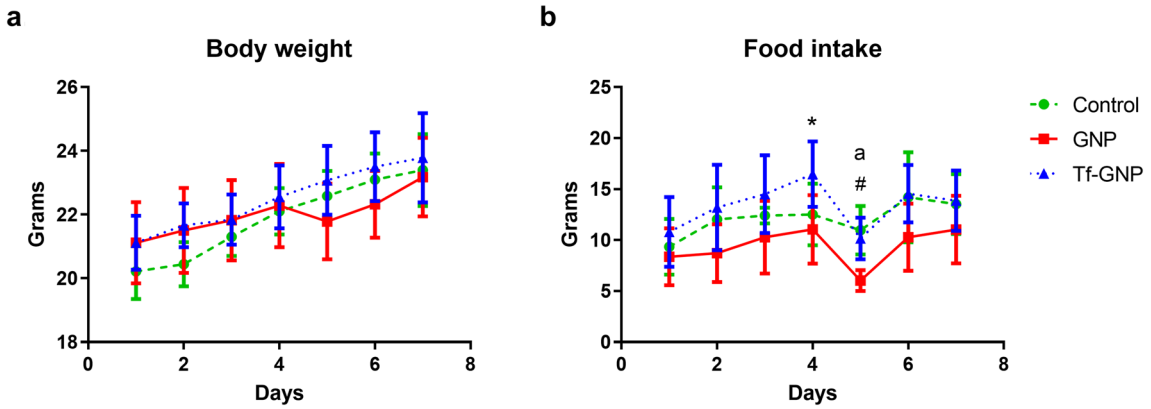

Fig. 7 Effect of bare GNP and Tf-GNP on **a** body weight and **b** food intake. Data are mean ± standard deviation S.D. (Statistical analysis: Two-way ANOVA followed by multiple comparison test. $^{*}p < 0.05$ (GNP vs. Tf-GNP), $^{\#}p < 0.05$ (Control vs. GNP) and $^{a}p < 0.05$ (Tf-GNP on day 4 vs. day 5))

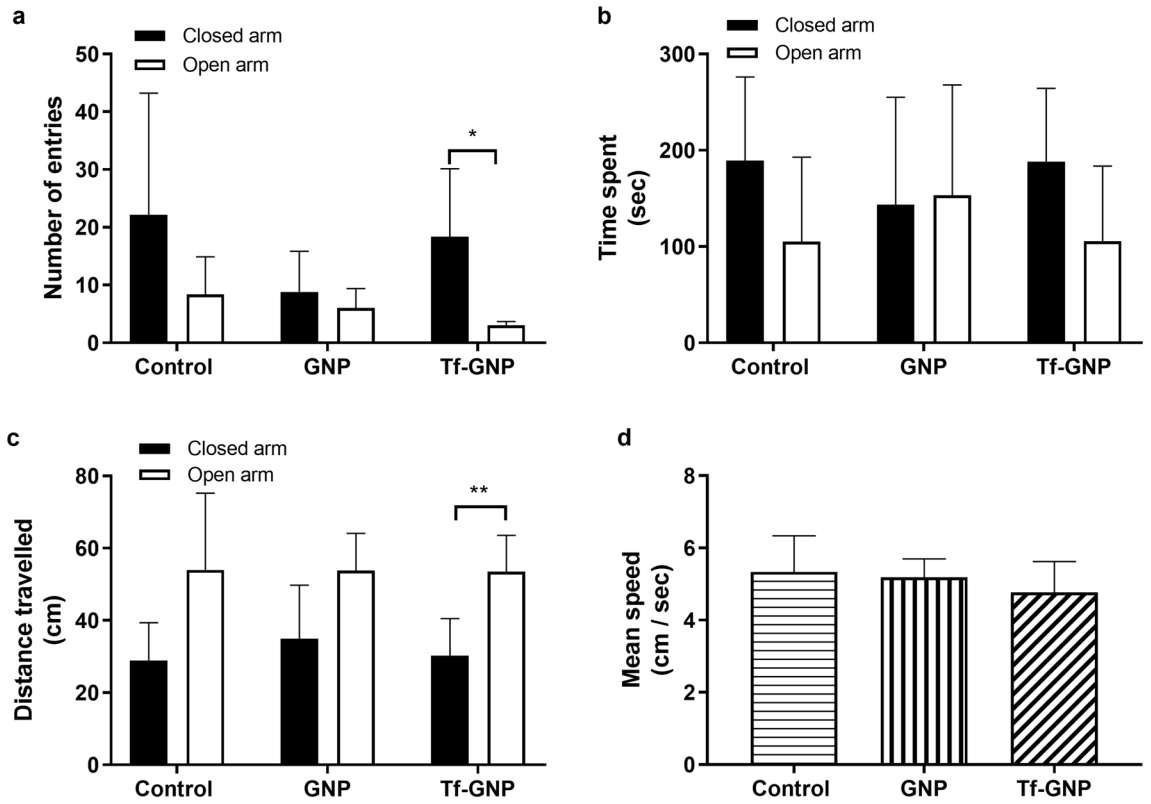

Fig. 8 Effect of bare GNP and Tf-GNP on **a** number of entries into closed and open arms, **b** time spent in closed and open arms, **c** distance traveled in closed and open arms and **d** mean speed in EPM. Data are mean ± standard deviation. (Statistical analyses: For the panels **a**, **b** and **c**, Student's paired t-test was performed ($^{*}p = 0.05$ and $^{**}p = 0.005$). For panel **d**, One-way ANOVA followed by Tukey's multiple comparison test was performed.) Black and white bars belong to the measurements in closed and open arms, respectively

observed at 1663 cm-1 compared to bare GNPs. In the literature, Tf-conjugated NPs do not show a distinct band upon conjugation but a slight increase in Amide band was reported [45]. As a result, the DLS, TEM and FTIR results support the conjugation of Tf presence. Similarly, in literature DLS and TEM results are also used to demonstrate the confirmation of conjugation [46, 47].

Various strategies have been developed to assist the nanoparticles to cross the BBB. Previous studies indicated that bio-distribution of GNPs in various organs is size-dependent

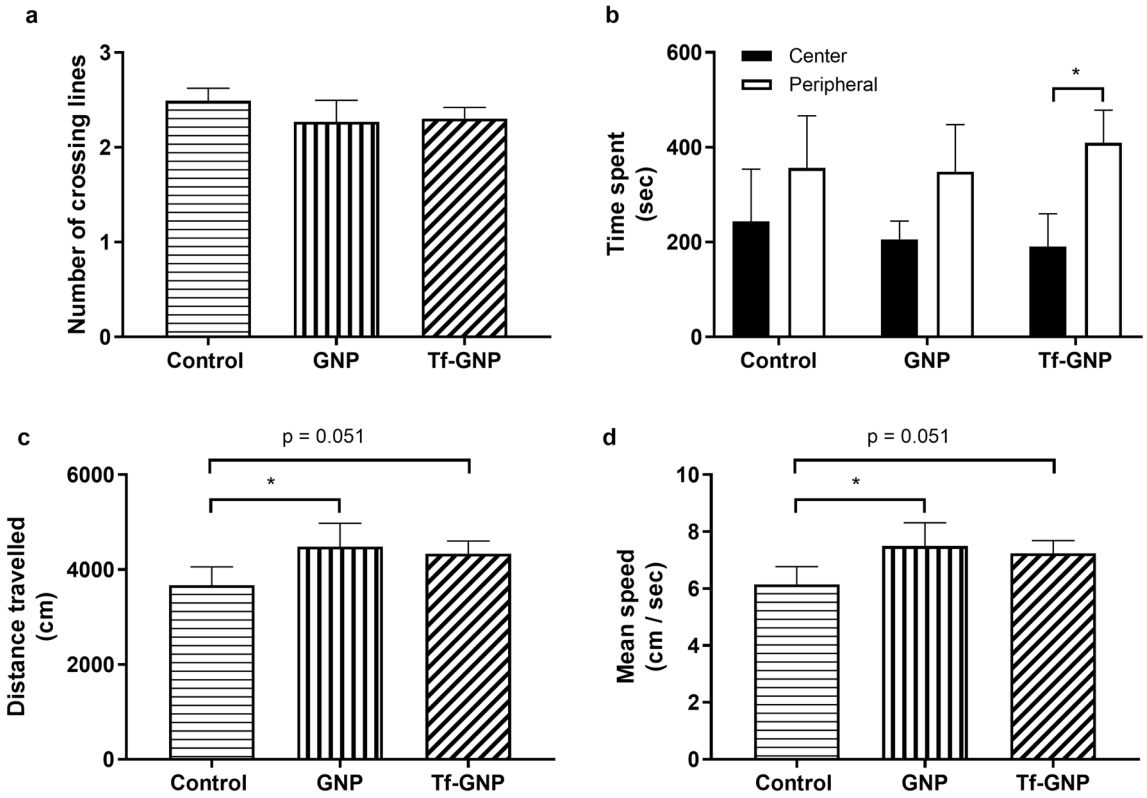

Fig. 9 Effect of bare GNP and Tf-GNP on **a** number crossing lines, **b** time spent in central and peripheral zones, **c** total distance traveled in both zones and **d** mean speed in OFT. Data are mean ± standard deviation. (Statistical analyses: For the panels **a**, **c** and **d**, One-way ANOVA followed by Tukey's multiple comparison test was performed ($*p < 0.02$). For panel **b**, Student's paired *t*-test (for control and Tf-GNP groups) and Wilcoxon matched-pair signed rank test (for GNP group) were performed ($*p < 0.05$).) Black and white bars belong to the measurements in central and peripheral zones, respectively

[48–52]. Moreover, surface modifications can also alter the biodistribution [53, 54] and toxicity [55, 56] of GNPs. A recent study investigated the polyethylene glycol-modified GNPs (PEGylated NPs) nd compared their electrophysiological effects on hippocampal neurons ex vivo and reported hat treatment with PEGylated GNPs led to similar electrophysiological characteristics in hippocampal neurons with untreated group [44]. In our study, the spontaneous firing rate observed for the neurons treated with bare GNPs were same in the neurons treated with Tf-GNPs. Moreover, GNPs were shown to be beneficial in neural injuries such in spinal cord injury when PEGylated [57] and sciatic nerve injury when conjugated with chitosan [58].

The dose applied in this study is below the toxic levels of bare GNPs on neural cells but reported to cause neuronal functional toxicity [43, 44, 59]. Since low doses were administered to the mice in the current study, it is expected to have similar amount of transferee to the brain both for bare GNP and for Tf-GNP as shown with ICP-MS results. Bare GNPs in brain of mice after three days injection were increased the firing frequency of hippocampal neurons in line with the results both reported by our group and other groups [43, 44, 59]. However, Tf conjugated GNPs having similar brain dose with the bare GNPs shown by ICP-MS resulted no change in spontaneous firing frequency of hippocampal neurons.

In our study, administration of Tf-GNPs for three consecutive days led to increase in the anxiety-like behavior without having any effect on locomotion in vivo. Previously, zinc oxide [60, 61] and magnesium oxide [62] nanoparticles were shown to have anxiolytic effects in rodents, while silica nanoparticles were found to be anxiogenic in adult zebrafish [63]. On the other hand, neither bare nor PEGylated GNPs were found to alter the behavior in terms of anxiety in mice [44]. Various regions and neural pathways are involved in brain modulating anxiety behavior [64, 65]. Hippocampus is one of the regions playing role in anxiety [66, 67] and inputs from hippocampus to other brain regions including lateral septum [68] medial frontal cortex [69] and lateral hypothalamus [68] regulate anxiety. On the other hand, other regions including amygdala [66] and bed nucleus of the stria terminalis [70] and the neural circuitries between other regions of the brain have been implicated to play roles in the regulation of anxiety [71, 72]. Although the effect of nanoparticles on

hippocampal neuronal activity has been studied in various the studies, the activity of the neurons and possible alterations in the abovementioned circuits should be also investigated to elucidate impact of the bare and conjugated GNPs on anxiety behavior in transgenic mice using methods such as optogenetics [68].

Conclusions

Bare GNPs, but not the Tf-GNPs, elevated the spontaneous firing frequency of hippocampal neurons ex vivo. On the other hand, Tf-GNPs elevated the anxiety-like behavior without altering the locomotor activity in vivo. The exact mechanisms of conjugated GNPs, in this specific case, Tf-GNPs, on the effect of neuronal activity remain to be elusive. Moreover, effects of these nanoparticles on brain chemistry and plasticity are still unknown. Studies investigating such effects with different conjugation methods and materials may be beneficial for the improvements in applications of GNPs for neurological conditions.

Acknowledgements None.

Author contributions YY performed behavioral experiments and electrophysiological recordings; GY performed synthesis of gold nanoparticles and characterization; BGT performed characterization of gold nanoparticles, analyzed, and interpret the data; BGT, GAG, AM, and MC provided technical support, reagents, and instrumentation; BY conceived experiments, analyzed data, prepared figures, and wrote the paper.

Funding This study did not receive any grants from any third parties.

Data availability Not applicable.

Declarations

Conflict of interest The authors declare that they have no conflict of interests.

Ethical approval This study was performed in line with the principles of the Declaration of Helsinki. Approval was granted by the Ethics Committee of Yeditepe University on Experimental Animal Research (Date. 17/03/2017 /No: 599).

References

1. Singh P, Pandit S, Mokkapati V, Garg A, Ravikumar V, Mijakovic I (2018) Gold nanoparticles in diagnostics and therapeutics for human cancer. Int J Mol Sci. https://doi.org/10.3390/ijms19071979
2. Wang S and Lu G (2018) Applications of gold nanoparticles in cancer imaging and treatment. In: Seehra MS, Bristow AD (eds) Noble and precious metals—properties, nanoscale effects and applications. pp 291–309
3. Siddique S, Chow JCL (2020) Application of nanomaterials in biomedical imaging and cancer therapy. Nanomaterials (Basel). https://doi.org/10.3390/nano10091700
4. Emami T, Madani R, Golchinfar F, Shoushtary A, Amini SM (2015) Comparison of gold nanoparticle conjugated secondary antibody with non-gold secondary antibody in an ELISA kit model. Monoclon Antib Immunodiagn Immunother 34:366–370. https://doi.org/10.1089/mab.2015.0021
5. Davatgaran Taghipour Y, Kharrazi S, Amini SM (2018) Antibody conjugated gold nanoparticles for detection of small amounts of antigen based on surface plasmon resonance (SPR) spectra. Nanomed Res J 3:102–108
6. Fatemi F, Amini SM, Kharrazi S, Rasaee MJ, Mazlomi MA, Asadi-Ghalehni M, Rajabibazl M, Sadroddiny E (2017) Construction of genetically engineered M13K07 helper phage for simultaneous phage display of gold binding peptide 1 and nuclear matrix protein 22 ScFv antibody. Colloids Surf B 159:770–780. https://doi.org/10.1016/j.colsurfb.2017.08.034
7. Rezaeian A, Amini SM, Najafabadi MRH, Farsangi ZJ, Samadian H (2022) Plasmonic hyperthermia or radiofrequency electric field hyperthermia of cancerous cells through green-synthesized curcumin-coated gold nanoparticles. Lasers Med Sci 37:1333–1341. https://doi.org/10.1007/s10103-021-03399-7
8. Amini SM, Kharrazi S, Rezayat SM, Gilani K (2018) Radiofrequency electric field hyperthermia with gold nanostructures: role of particle shape and surface chemistry. Artif Cell Nanomedi Biotechnol 46:1452–1462
9. Vines JB, Yoon J-H, Ryu N-E, Lim D-J, Park H (2019) Gold nanoparticles for photothermal cancer therapy. Front Chem 7:167
10. Chen Y, Yang J, Fu S, Wu J (2020) Gold nanoparticles as radiosensitizers in cancer radiotherapy. Int J Nanomed 15:9407–9430. https://doi.org/10.2147/ijn.S272902
11. Haume K, Rosa S, Grellet S, Śmiałek MA, Butterworth KT, Solov'yov AV, Prise KM, Golding J, Mason NJ (2016) Gold nanoparticles for cancer radiotherapy: a review. Cancer Nanotechnol 7:8. https://doi.org/10.1186/s12645-016-0021-x
12. Cheng Y, A CS, Meyers JD, Panagopoulos I, Fei B and Burda C, (2008) Highly efficient drug delivery with gold nanoparticle vectors for in vivo photodynamic therapy of cancer. J Am Chem Soc 130:10643–10647. https://doi.org/10.1021/ja801631c
13. Tao Y, Li M, Ren J, Qu X (2015) Metal nanoclusters: novel probes for diagnostic and therapeutic applications. Chem Soc Rev 44:8636–8663. https://doi.org/10.1039/c5cs00607d
14. Stafstrom CE, Carmant L (2015) Seizures and epilepsy: an overview for neuroscientists. Cold Spring Harb Perspect Med. https://doi.org/10.1101/cshperspect.a022426
15. Wada A (2006) Roles of voltage-dependent sodium channels in neuronal development, pain, and neurodegeneration. J Pharmacol Sci 102:253–268. https://doi.org/10.1254/jphs.crj06012x
16. Imbrici P, Camerino DC, Tricarico D (2013) Major channels involved in neuropsychiatric disorders and therapeutic perspectives. Front Genet 4:76. https://doi.org/10.3389/fgene.2013.00076
17. Yilmaz B, Gilmore D, Wilson C (1996) Inhibition of the preovulatory LH surge in the rat by central noradrenergic mediation: involvement of an anaesthetic (urethane) and opioid receptor agonists. Biog Amin 12:423–435
18. Kutlu S, Yilmaz B, Canpolat S, Sandal S, Ozcan M, Kumru S, Kelestimur H (2004) Mu opioid modulation of oxytocin secretion in late pregnant and parturient rats. Involv Noradrenergic Neurotransm Neuroendocrinol 79:197–203. https://doi.org/10.1159/000078101
19. Ozcan M, Yilmaz B, King WM, Carpenter DO (2004) Hippocampal long-term potentiation (LTP) is reduced by a coplanar PCB congener. Neurotoxicology 25:981–988. https://doi.org/10.1016/j.neuro.2004.03.014

20. Taskin IC, Sen O, Emanet M, Culha M, Yilmaz B (2020) Hexagonal boron nitrides reduce the oxidative stress on cells. Nanotechnology 31:215101. https://doi.org/10.1088/1361-6528/ab6fdc
21. Paviolo C, Stoddart PR (2017) Gold nanoparticles for modulating neuronal behavior. Nanomaterials (Basel). https://doi.org/10.3390/nano7040092
22. Upadhyay RK (2014) Drug delivery systems, CNS protection, and the blood brain barrier. Biomed Res Int 2014:869269. https://doi.org/10.1155/2014/869269
23. Jones AR, Shusta EV (2007) Blood-brain barrier transport of therapeutics via receptor-mediation. Pharm Res 24:1759–1771. https://doi.org/10.1007/s11095-007-9379-0
24. Kutlu S, Aydin M, Alcin E, Ozcan M, Bakos J, Jezova D, Yilmaz B (2010) Leptin modulates noradrenaline release in the paraventricular nucleus and plasma oxytocin levels in female rats: a microdialysis study. Brain Res 1317:87–91. https://doi.org/10.1016/j.brainres.2009.12.044
25. Kawabata H (2019) Transferrin and transferrin receptors update. Free Radic Biol Med 133:46–54. https://doi.org/10.1016/j.freeradbiomed.2018.06.037
26. Pulgar VM (2018) Transcytosis to cross the blood brain barrier. New Adv Chall Front Neurosci 12:1019. https://doi.org/10.3389/fnins.2018.01019
27. Funabashi T, Suyama K, Uemura T, Hirose M, Hirahara F, Kimura F (2001) Immortalized gonadotropin-releasing hormone neurons (GT1-7 cells) exhibit synchronous bursts of action potentials. Neuroendocrinology 73:157–165. https://doi.org/10.1159/000054632
28. Strober W (2001) Trypan blue exclusion test of cell viability. Curr Protoc Immunol Appendix. https://doi.org/10.1002/0471142735.ima03bs21
29. Aklan I, Sayar Atasoy N, Yavuz Y, Ates T, Coban I, Koksalar F, Filiz G, Topcu IC, Oncul M, Dilsiz P, Cebecioglu U, Alp MI, Yilmaz B, Davis DR, Hajdukiewicz K, Saito K, Konopka W, Cui H, Atasoy D (2020) NTS catecholamine neurons mediate hypoglycemic hunger via medial hypothalamic feeding pathways. Cell Metab 31:313-326.e5. https://doi.org/10.1016/j.cmet.2019.11.016
30. Lezak KR, Missig G, Carlezon WA Jr (2017) Behavioral methods to study anxiety in rodents. Dialogues Clin Neurosci 19:181–191. https://doi.org/10.31887/DCNS.2017.19.2/wcarlezon
31. Seibenhener ML, Wooten MC (2015) Use of the open field maze to measure locomotor and anxiety-like behavior in mice. J Vis Exp. https://doi.org/10.3791/52434
32. Amini SM, Kharrazi S, Hadizadeh M, Fateh M, Saber R (2013) Effect of gold nanoparticles on photodynamic efficiency of 5-aminolevolenic acid photosensitiser in epidermal carcinoma cell line: an in vitro study. IET Nanobiotechnol 7:151–156. https://doi.org/10.1049/iet-nbt.2013.0021
33. Badirzadeh A, Alipour M, Najm M, Vosoogh A, Vosoogh M, Samadian H, Hashemi AS, Farsangi ZJ, Amini SM (2022) Potential therapeutic effects of curcumin coated silver nanoparticle in the treatment of cutaneous leishmaniasis due to Leishmania major in-vitro and in a murine model. J Drug Deliv Sci Technol 74:103576. https://doi.org/10.1016/j.jddst.2022.103576
34. Repar N, Li H, Aguilar JS, Li QQ, Drobne D, Hong Y (2018) Silver nanoparticles induce neurotoxicity in a human embryonic stem cell-derived neuron and astrocyte network. Nanotoxicology 12:104–116. https://doi.org/10.1080/17435390.2018.1425497
35. Engin AB, Engin A (2019) Nanoparticles and neurotoxicity: dual response of glutamatergic receptors. Prog Brain Res 245:281–303. https://doi.org/10.1016/bs.pbr.2019.03.005
36. Yousef MI, Abuzreda AA, Kamel MA (2019) Neurotoxicity and inflammation induced by individual and combined exposure to iron oxide nanoparticles and silver nanoparticles. J Taibah Univ Sci 13:570–578. https://doi.org/10.1080/16583655.2019.1602351
37. Shukla R, Bansal V, Chaudhary M, Basu A, Bhonde RR, Sastry M (2005) Biocompatibility of gold nanoparticles and their endocytotic fate inside the cellular compartment: a microscopic overview. Langmuir 21:10644–10654. https://doi.org/10.1021/la0513712
38. Adewale OB, Davids H, Cairncross L, Roux S (2019) Toxicological behavior of gold nanoparticles on various models: influence of physicochemical properties and other factors. Int J Toxicol 38:357–384. https://doi.org/10.1177/1091581819863130
39. Flora SJS (2017) Chapter 8—the applications, neurotoxicity, and related mechanism of gold nanoparticles. In: Jiang X, Gao H (eds) Neurotoxicity of nanomaterials and nanomedicine. Academic Press, pp 179–203
40. Velasco-Aguirre C, Morales F, Gallardo-Toledo E, Guerrero S, Giralt E, Araya E, Kogan MJ (2015) Peptides and proteins used to enhance gold nanoparticle delivery to the brain: preclinical approaches. Int J Nanomed 10:4919–4936. https://doi.org/10.2147/ijn.s82310
41. Dante S, Petrelli A, Petrini EM, Marotta R, Maccione A, Alabastri A, Quarta A, De Donato F, Ravasenga T, Sathya A, Cingolani R, Proietti Zaccaria R, Berdondini L, Barberis A, Pellegrino T (2017) Selective targeting of neurons with inorganic nanoparticles: revealing the crucial role of nanoparticle surface charge. ACS Nano 11:6630–6640. https://doi.org/10.1021/acsnano.7b00397
42. Salinas K, Kereselidze Z, DeLuna F, Peralta XG, Santamaria F (2014) Transient extracellular application of gold nanostars increases hippocampal neuronal activity. J Nanobiotechnology 12:31. https://doi.org/10.1186/s12951-014-0031-y
43. Tuna BG, Yavuz Y, Kuku G, Maharramov A, Yilmaz B, Saricam M, Ercan M, Culha M, Dogan S (2019) The effect of modified gold nanoparticles on the function of neurons of mice hippocampal brain slices. Mersin Univ Saglık Bilim Derg 12:328–340
44. Tuna BG, Yesilay G, Yavuz Y, Yilmaz B, Culha M, Maharramov A, Dogan S (2020) Electrophysiological effects of polyethylene glycol modified gold nanoparticles on mouse hippocampal neurons. Heliyon 6:e05824. https://doi.org/10.1016/j.heliyon.2020.e05824
45. Soe ZC, Kwon JB, Thapa RK, Ou W, Nguyen HT, Gautam M, Oh KT, Choi HG, Ku SK, Yong CS, Kim JO (2019) Transferrin-conjugated polymeric nanoparticle for receptor-mediated delivery of doxorubicin in doxorubicin-resistant breast cancer cells. Pharmaceutics. https://doi.org/10.3390/pharmaceutics11020063
46. Lopes Rodrigues R, Xie F, Porter AE, Ryan MP (2020) Geometry-induced protein reorientation on the spikes of plasmonic gold nanostars. Nanoscale Adv 2:1144–1151. https://doi.org/10.1039/c9na00584f
47. Li JL, Wang L, Liu XY, Zhang ZP, Guo HC, Liu WM, Tang SH (2009) In vitro cancer cell imaging and therapy using transferrin-conjugated gold nanoparticles. Cancer Lett 274:319–326. https://doi.org/10.1016/j.canlet.2008.09.024
48. De Jong WH, Hagens WI, Krystek P, Burger MC, Sips AJ, Geertsma RE (2008) Particle size-dependent organ distribution of gold nanoparticles after intravenous administration. Biomaterials 29:1912–1919. https://doi.org/10.1016/j.biomaterials.2007.12.037
49. Semmler-Behnke M, Kreyling WG, Lipka J, Fertsch S, Wenk A, Takenaka S, Schmid G, Brandau W (2008) Biodistribution of 1.4- and 18-nm gold particles in rats. Small 4:2108–2111. https://doi.org/10.1002/smll.200800922
50. Sonavane G, Tomoda K, Makino K (2008) Biodistribution of colloidal gold nanoparticles after intravenous administration: effect of particle size. Colloids Surf B 66:274–280. https://doi.org/10.1016/j.colsurfb.2008.07.004
51. Lasagna-Reeves C, Gonzalez-Romero D, Barria MA, Olmedo I, Clos A, Sadagopa Ramanujam VM, Urayama A, Vergara L, Kogan MJ, Soto C (2010) Bioaccumulation and toxicity of gold

nanoparticles after repeated administration in mice. Biochem Biophys Res Commun 393:649–655. https://doi.org/10.1016/j.bbrc.2010.02.046
52. Hirn S, Semmler-Behnke M, Schleh C, Wenk A, Lipka J, Schäffler M, Takenaka S, Möller W, Schmid G, Simon U, Kreyling WG (2011) Particle size-dependent and surface charge-dependent biodistribution of gold nanoparticles after intravenous administration. Eur J Pharm Biopharm 77:407–416. https://doi.org/10.1016/j.ejpb.2010.12.029
53. Takeuchi I, Onaka H, Makino K (2018) Biodistribution of colloidal gold nanoparticles after intravenous injection: effects of PEGylation at the same particle size. Biomed Mater Eng 29:205–215. https://doi.org/10.3233/bme-171723
54. Terentyuk GS, Maslyakova GN, Suleymanova LV, Khlebtsov BN, Kogan BY, Akchurin GG, Shantrocha AV, Maksimova IL, Khlebtsov NG, Tuchin VV (2009) Circulation and distribution of gold nanoparticles and induced alterations of tissue morphology at intravenous particle delivery. J Biophotonics 2:292–302. https://doi.org/10.1002/jbio.200910005
55. Pan Y, Leifert A, Ruau D, Neuss S, Bornemann J, Schmid G, Brandau W, Simon U, Jahnen-Dechent W (2009) Gold nanoparticles of diameter 1.4 nm trigger necrosis by oxidative stress and mitochondrial damage. Small 5:2067–2076. https://doi.org/10.1002/smll.200900466
56. Simpson CA, Salleng KJ, Cliffel DE, Feldheim DL (2013) In vivo toxicity, biodistribution, and clearance of glutathione-coated gold nanoparticles. Nanomedicine 9:257–263. https://doi.org/10.1016/j.nano.2012.06.002
57. Papastefanaki F, Jakovcevski I, Poulia N, Djogo N, Schulz F, Martinovic T, Ciric D, Loers G, Vossmeyer T, Weller H, Schachner M, Matsas R (2015) Intraspinal delivery of polyethylene glycol-coated gold nanoparticles promotes functional recovery after spinal cord injury. Mol Ther 23:993–1002. https://doi.org/10.1038/mt.2015.50
58. Lin YL, Jen JC, Hsu SH, Chiu IM (2008) Sciatic nerve repair by microgrooved nerve conduits made of chitosan-gold nanocomposites. Surg Neurol 70(S1):9–18. https://doi.org/10.1016/j.surneu.2008.01.057
59. Jung S, Bang M, Kim BS, Lee S, Kotov NA, Kim B, Jeon D (2014) Intracellular gold nanoparticles increase neuronal excitability and aggravate seizure activity in the mouse brain. PLoS ONE 9:e91360. https://doi.org/10.1371/journal.pone.0091360
60. Xie Y, Wang Y, Zhang T, Ren G, Yang Z (2012) Effects of nanoparticle zinc oxide on spatial cognition and synaptic plasticity in mice with depressive-like behaviors. J Biomed Sci 19:14. https://doi.org/10.1186/1423-0127-19-14
61. Torabi M, Kesmati M, Harooni HE, Varzi HN (2013) Effects of nano and conventional zinc oxide on anxiety-like behavior in male rats. Indian J Pharmacol 45:508–512. https://doi.org/10.4103/0253-7613.117784
62. Kesmati M, Torabi M, Teymuri Zamaneh H, Malekshahi Nia H (2014) Interaction between anxiolytic effects of magnesium oxide nanoparticles and exercise in adult male rat. Nanomed J 1:324–330. https://doi.org/10.7508/nmj.2015.05.006
63. Li X, Liu X, Li T, Li X, Feng D, Kuang X, Xu J, Zhao X, Sun M, Chen D, Zhang Z, Feng X (2017) SiO_2 nanoparticles cause depression and anxiety-like behavior in adult zebrafish. RSC Adv 7:2953–2963. https://doi.org/10.1039/C6RA24215D
64. Martin EI, Ressler KJ, Binder E, Nemeroff CB (2009) The neurobiology of anxiety disorders: brain imaging, genetics, and psychoneuroendocrinology. Psychiatr Clin North Am 32:549–575. https://doi.org/10.1016/j.psc.2009.05.004
65. Duval ER, Javanbakht A, Liberzon I (2015) Neural circuits in anxiety and stress disorders: a focused review. Ther Clin Risk Manag 11:115–126. https://doi.org/10.2147/tcrm.s48528
66. McHugh SB, Deacon RM, Rawlins JN, Bannerman DM (2004) Amygdala and ventral hippocampus contribute differentially to mechanisms of fear and anxiety. Behav Neurosci 118:63–78. https://doi.org/10.1037/0735-7044.118.1.63
67. Revest JM, Dupret D, Koehl M, Funk-Reiter C, Grosjean N, Piazza PV, Abrous DN (2009) Adult hippocampal neurogenesis is involved in anxiety-related behaviors. Mol Psychiatry 14:959–967. https://doi.org/10.1038/mp.2009.15
68. Jimenez JC, Su K, Goldberg AR, Luna VM, Biane JS, Ordek G, Zhou P, Ong SK, Wright MA, Zweifel L, Paninski L, Hen R, Kheirbek MA (2018) Anxiety cells in a hippocampal-hypothalamic circuit. Neuron 97:670-683.e6. https://doi.org/10.1016/j.neuron.2018.01.016
69. Adhikari A, Topiwala MA, Gordon JA (2011) Single units in the medial prefrontal cortex with anxiety-related firing patterns are preferentially influenced by ventral hippocampal activity. Neuron 71:898–910. https://doi.org/10.1016/j.neuron.2011.07.027
70. Kim SY, Adhikari A, Lee SY, Marshel JH, Kim CK, Mallory CS, Lo M, Pak S, Mattis J, Lim BK, Malenka RC, Warden MR, Neve R, Tye KM, Deisseroth K (2013) Diverging neural pathways assemble a behavioural state from separable features in anxiety. Nature 496:219–223. https://doi.org/10.1038/nature12018
71. Adhikari A (2014) Distributed circuits underlying anxiety. Front Behav Neurosci 8:112. https://doi.org/10.3389/fnbeh.2014.00112
72. Ahrens S, Wu MV, Furlan A, Hwang GR, Paik R, Li H, Penzo MA, Tollkuhn J, Li B (2018) A central extended amygdala circuit that modulates anxiety. J Neurosci 38:5567–5583. https://doi.org/10.1523/jneurosci.0705-18.2018